

Control of Flexibility and Pore Structure of Tetraethylorthosilicate/ Methyltriethoxysilane Aerogels by Hybridization[‡]

CHANG-YEOL KIM* and A. RUM JANG

Nano-IT Convergence Center, Korea Institute of Ceramic Engineering & Technology 233-5 Gasan-dong Geumcheon-gu, 153-801 Seoul, South Korea

*Corresponding author: Fax: +82 2 32827769; Tel: +82 2 3282-2427; E-mail: cykim15@kicet.re.kr

AJC-11357

We found that the flexibility, pore structures such as pore sizes, porosity and specific surface area could be controlled by changing ratio of tetraethylorthosilicate/methyltriethoxysilane (TEOS/MTEOS). A methyl functional group of MTEOS causes the difficulty of hydrolysis and condensation reactions, so that strong basic catalyst needs to be added for the gellation of MTEOS. Therefore, increasing of MTEOS ratio forms larger pore sizes and large primary particles with *ca.* 1 μm . MTEOS-based aerogels show the lowest specific area due to macropores with more than 1000 nm, although they are very flexible to elongate two times as long as their original sample length. For TEOS/MTEOS hybrid aerogels with 1:1 molar ratio, they have the largest specific surface area and pore volume, a little flexibility and hydrophobicity due to the remaining alkyl functional groups. This research presents the possibility of controlling flexibility, pore structures, hydrophobicity through hybridization of alkoxide and silane. It suggests a way of overcoming weaknesses of silica aerogels like brittleness and hydrophilicity.

Key Words: Flexibility, Pore structure, Hybrid, Aerogels, Hydrophobicity.

INTRODUCTION

Silica aerogel is the lightest solid material human developed due to its high porosity (more than 90 %), high specific area (*ca.* 1000 m^2/g) and small pore size (*ca.* 10 nm)¹⁻⁴. Since Kisley⁵ synthesized silica aerogel from sodium silicate, many researches have been conducted for the application of silica aerogels to thermal insulation, acoustic insulation, Cerenkov radiation detectors, low dielectric constant films in ultra large scale integrated circuits, superhydrophobic aerogels for oil-spill cleanup, catalysts and internal confinement fusion targets in thermonuclear fusion reactions⁶⁻⁹.

Although silica aerogel has many attractive properties such as high specific surface area, high pore volume and low thermal conductivity, its applications are limited due to its mechanical fragility and brittleness. Many researches are focused on finding a way to overcome the mechanical fragility. For example, silica aerogel and fiber composites have already commercialized by Aspen Aerogel Inc. The composition of silica aerogels and polymers has been tried to overcome the mechanical weaknesses¹⁰⁻¹⁴. Rao *et al.*^{15,16}, presented a new method to synthesize flexible aerogels using methyltrimethoxy silane (MTMS). The aerogels undergo 60 % compression by volume and regain their original dimensions after the applied stress is released.

However, they only presented transmission electron microscopy data to show the porous structure of MTMS aerogels, but did not show any nitrogen adsorption and desorption data. MTMS-based aerogels have been synthesized by controlling MTMS:methanol:H₂O ratio and an ambient drying method.

The interest of this paper is to control the flexibility, pore structures, hydrophobicity of aerogels by hybridization of alkoxide and silane. Organic functional groups in silane retard the hydrolysis and condensation reactions because of the limitations of reduced branches. For example, methyltriethoxysilane (MTEOS) we chose as a silane in this paper could be linked each other in three directions. So, we tried to find out the effects of monosilane and alkoxide composition to the flexibility and pore structures.

EXPERIMENTAL

Preparation of samples: Tetraethylorthosilicate (TEOS, Aldrich) sol was synthesized by adding TEOS into methanol and 5×10^{-4} M HCl as a catalyst. Tetraethylorthosilicate concentration was 1M and H₂O/TEOS molar ratio was 5. To gelate TEOS sol, 1M ammonium hydroxide was added to be pH 7. Methyltrimethoxy silane (Aldrich) sol was synthesized by adding H₂O and HCl to MTEOS for the hydrolysis reaction of MTEOS. The hydrolyzed MTMS was poured into methanol

[‡]Presented to The 5th Korea-China International Conference on Multi-Functional Materials and Application.

to be 1M H₂O/MTMS molar ratio was fixed at 5 and the concentration of HCl was 5×10^{-4} M. To gelate the MTMS sol needs strong basic conditions and so we added 10M ammonium hydroxide to be pH 10. The hybridization of TEOS/MTEOS was conducted by firstly mixing TEOS sol and MTEOS sol at one to one molar ratio. Although we varied TEOS:MTEOS ratio at 0:1, 0.2:8, 0.4:6, 0.5:0.5, 0.6:0.4, 0.8:0.2 and 1:0, we discussed the results of TEOS (the ratio at 1:0) and TEOS/MTEOS (0.5:0.5) and MTEOS (0:1), of which preparation conditions are summarized in Table-1. To synthesize TEOS/MTEOS hybrid aerogel, we first mixed TEOS sol and MTEOS sol at 50-50 vol % and 6M ammonium hydroxide was added at pH 8.5. The gellation of TEOS, TEOS/MTEOS and MTEOS sols was conducted at 65 °C and the gellation time varied between 4 and 24 h and it tended to take longer time with increasing MTEOS ratio. The gels were aged in methanol for 24 h at 50 °C.

To make aerogels, we adopted CO₂ supercritical drying method. The alcogels of TEOS, TEOS/MTEOS and MTEOS were placed into supercritical vessel at room temperature, solvent-exchanged by liquid CO₂ and then heated up to 40 °C and maintained at 9.5 MPa for 6 h. After drying, CO₂ pressure was released slowly for the aerogel samples not to be damaged.

Characterization of aerogels: We conducted a thermal analysis of the aerogels by differential thermal analysis (DTA) and thermogravimetry (TG). In order to investigate the hybridization of TEOS and MTEOS, Fourier-transformed infrared (FT-IR, Prestige, Shimadzu, Japan) spectroscopy and Raman scattering spectroscopy (NRS3000, Jasco, Japan) analyses were also conducted for TEOS, TEOS/MTEOS and MTEOS aerogel. The specific surface areas and pore size distributions of the aerogel composites were analyzed by the BET and BJH nitrogen gas absorption and desorption method (Tristar 3000, Micromeritics, USA). The apparent densities and porosities of the aerogels were analyzed by the Archimedes principle. The aerogel composites were hydrophobic, so ethanol (anhydrous, 99.9 %, d: 0.7896, Carlo Erba Co., Italy) was used for the density measurements. The contact angle (θ) measurements were performed using a contact angle meter (Phoenix 300 contact angle analyzer, SEO Corporation, South Korea) to quantify the degree of hydrophobicity.

RESULTS AND DISCUSSION

Chemical modification of TEOS/MTEOS hybrid aerogel: Fig. 1 shows FT-IR spectra of TEOS, TEOS/MTEOS and MTEOS-based silica aerogels. TEOS-based silica aerogel showed OH stretching and bending mode at 3434 and 1633 cm⁻¹, respectively. The bands of LO and TO asymmetric Si-O-Si stretching modes appeared at 1209 and 1075 cm⁻¹ respectively¹⁷⁻²², Si-O-Si stretching or vibration modes of ring structures appeared

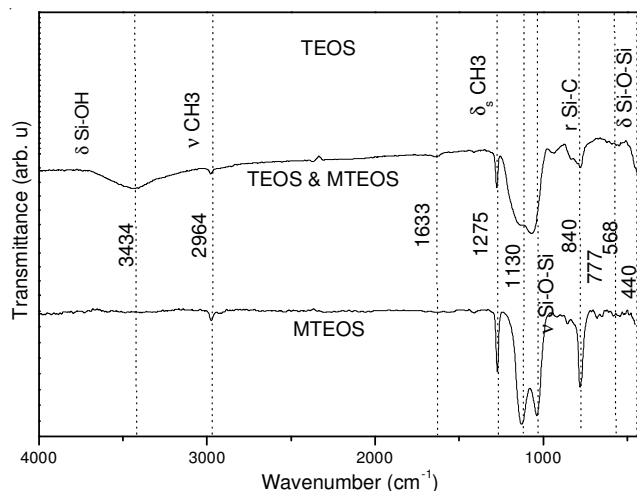


Fig. 1. FT-IR of TEOS, TEOS/MTEOS and MTEOS-based silica aerogels

at 777 cm⁻¹. The band at 440 cm⁻¹ is assigned to Si-O-Si bending modes and the absorption peak at 962 cm⁻¹ was attributed to Si-OH mode²². MTEOS-based aerogel, Si-CH₃ and Si-C mode appeared at 777, 840 and 1275 cm⁻¹. The vibration modes of CH₃ appeared at 2930 and 2964 cm⁻¹. There is no OH vibration mode for MTEOS-based aerogel. When we synthesized TEOS/MTEOS hybrid aerogel, we could find that Si-C modes at 770, 840 and 1275 cm⁻¹ and the absorption peak intensities of OH vibration and bending mode decreased, compared to those of TEOS-based silica aerogel.

Raman scattering spectra of TEOS, TEOS/MTEOS, MTEOS-based aerogels were shown in Fig. 2. The modes at 455, 302 and 210 cm⁻¹ are assigned to ring breathing of (SiO)_n and the vibration at 735 cm⁻¹ is assigned to $\rho(\text{CH}_3)$ and the peak at 796 cm⁻¹ is attributed to $\delta_{\text{sym}}(\text{Si-O-Si})$ ^{19,24,25}. The broad peaks at 1240 and 1420 cm⁻¹ are assigned to $\delta_{\text{sym}}(\text{CH}_3)$ and $\delta_{\text{asym}}(\text{CH}_3)$. For TEOS-based silica aerogel, there appeared no peaks which resulted from (CH₃) modes. However, we could find that the hybridization of TEOS and MTEOS were confirmed by the appearance of (CH₃) modes for TEOS/MTEOS aerogel samples.

DTA/TG thermal analyses: Fig. 4 shows the DTA and TG analyses of TEOS, TEOS/MTEOS and MTEOS aerogels. TEOS-based silica aerogel showed the sharp exothermic peak at 274 °C, accompanying 1 % of weight loss, which is due to the evaporation of the residual solvent and water molecules from the aerogel. The sharp decline in the weight observed at 410 °C accompanied by an exothermic peak in the DTA curve is due to the oxidation of the methyl groups responsible for the aerogel hydrophobicity. MTEOS-based aerogel showed two exothermic peaks at 386 and 486 °C, which is due to the oxidation of methyl functional groups in MTEOS accompanying 12 % of weight loss. TEOS/MTEOS hybrid aerogels

TABLE-1
EXPERIMENTAL CONDITIONS OF TEOS, TEOS/MTEOS AND MTEOS

Sample	Items					
	TEOS/MTEOS mole ratio	H ₂ O/TEOS or MTEOS	SiO ₂ concentration (M)	HCl 10 ⁻⁴ (mol)	NH ₄ OH concentration (M)	pH for gellation
TEOS	1:0	5	1	5	1	7
TEOS/MTEOS	0.5:0.5	5	1	5	6	8.5
MTEOS	0:1	5	1	5	10	10

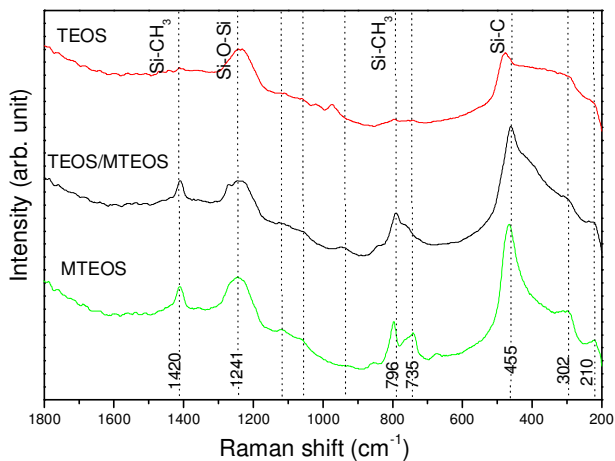
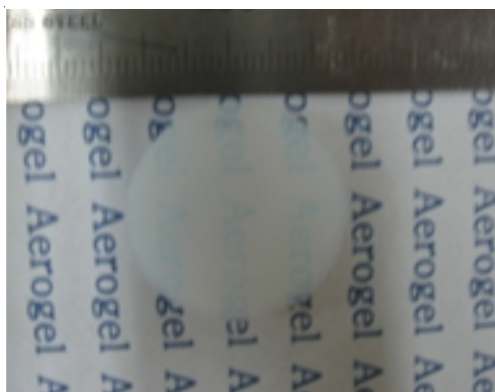


Fig. 2. Raman scattering spectra of TEOS, TEOS/MTEOS and MTEOS-based silica aerogels



(a)

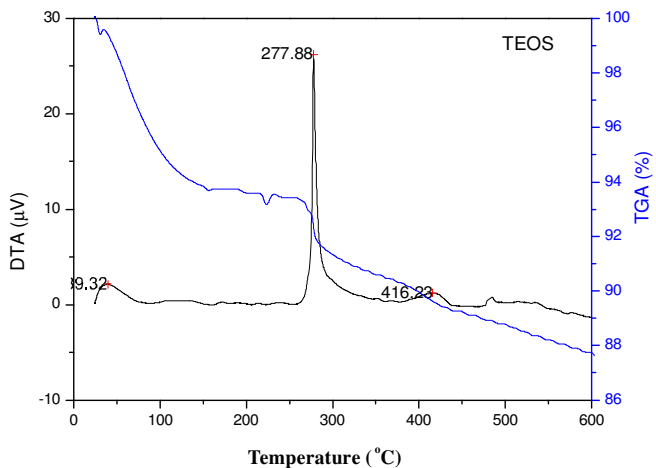


(b)

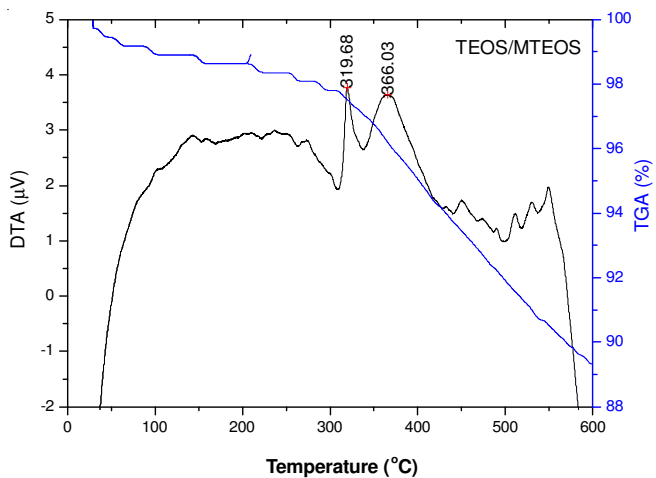


(c)

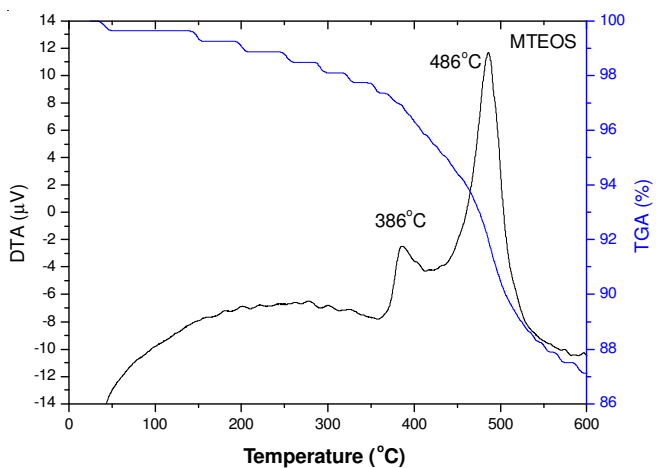
Fig. 3. Samples of TEOS, TEOS/MTEOS and MTEOS-based silica aerogels



(a)



(b)



(c)

Fig. 4. DTA/TG analysis of TEOS, TEOS/MTEOS and MTEOS-based silica aerogels

showed the two exothermic peaks at 320 and 366 °C, which are thought to result from the oxidation of methyl functional groups. The hybridization of MTEOS confers the hydrophobicity and flexibility of aerogels. It is known that the hydrophobicity and flexibility of aerogels remains to 450 °C¹⁶.

Nitrogen gas adsorption and desorption: We analyzed the nitrogen gas adsorption and desorption characteristics of TEOS, TEOS/MTEOS and MTEOS aerogels (Fig. 5). TEOS-

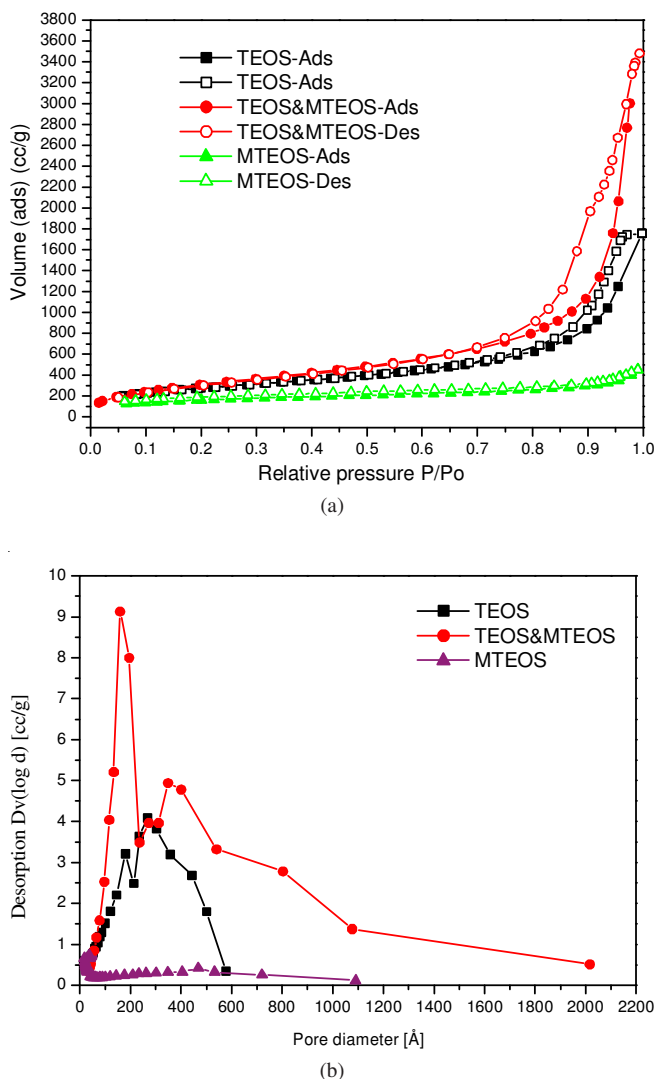


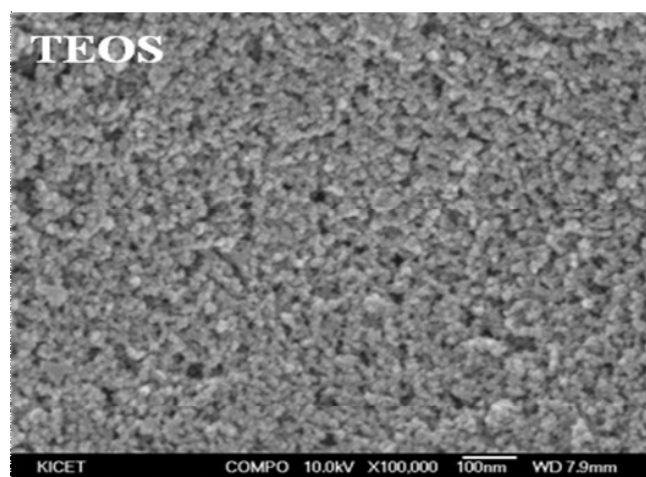
Fig. 5. Isotherm graphs (a) and pore diameter distributions (b) of TEOS, TEOS/MTEOS and MTEOS-based silica aerogels by N_2 adsorption and desorption

based silica aerogels, showed type IV mesoporous nitrogen adsorption and desorption characteristics. The adsorption of nitrogen gas into TEOS aerogel increased linearly with relative pressure and the increasing curve showed S shape between 0.7 and 1.0 relative pressure range. The maximum adsorption volume of nitrogen gas was 1600 cc/g for TEOS-based aerogel. When we prepared TEOS/MTEOS composite aerogel, it showed a little different aspect of nitrogen gas adsorption and desorption isotherms. Firstly, the maximum adsorption value of nitrogen gas into TEOS/MTEOS increased to 3400 cc/g. The desorption of adsorbed nitrogen gases occurred *via* two steps, which means that the pore distributions are comprised of two different-diameter pores, the larger ones and the smaller ones. MTEOS-based aerogel showed the lowest adsorption

volume, which indicates that the mesopore volume is small, compared to another TEOS and TEOS/MTEOS aerogels. The pore size distributions showed that TEOS-based silica aerogel is comprised of mesopores with 10-500 Å, with mean diameter of around 300 Å. The pore diameter distributions of TEOS/MTEOS-based aerogels showed two peaks at about 160 and 400 Å. We observed that MTEOS-based aerogels are comprised of very small sized pores with less than 50 Å.

Table-2 summarized the properties of TEOS, TEOS/MTEOS and MTEOS-based aerogels. TEOS-based silica aerogel showed the density of 0.123 g/cm³ and about 90 % of porosity, 1016 m²/g of specific surface area and its pore volume of 2.67 cc/g and 266 Å of pore diameter. MTEOS-based aerogels showed the higher specific surface area, 586 m²/g and pore volume, 0.56 cc/g and 58 Å of pore diameter. The density and porosity of MTEOS-based aerogels were 0.066 g/cm³ and 94.7 %, respectively. When we hybridized TEOS and MTEOS, we could find that the specific surface area increased to 1165 m²/g and the pore volume was 5.37 cc/g and pore diameter, 160 Å. The density of TEOS/MTEOS was 0.104 cm³/g and the porosity was 91.80 %.

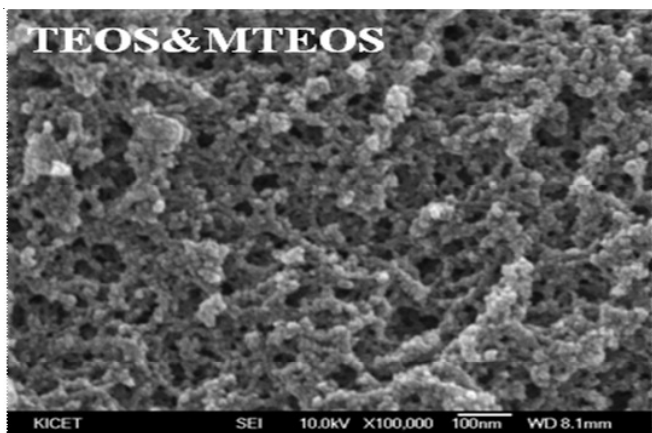
Microstructure observations: FESEM images of TEOS, TEOS/MTEOS and MTEOS-based aerogels were observed, as is shown in Fig. 6. TEOS-based aerogels showed that the microstructures are comprised of the three dimensional networks of ten nanometer-sized silica nano-particles, forming *ca.* 10 nm sized pores. For TEOS/MTEOS-based hybrid aerogels, the pores are comprised of small pores with 10 nm in diameter and large pores with about 50 nm in diameter. MTEOS-based aerogels showed quite a different microstructures which are comprised of the networks of clusters with about hundreds nanometer. The clusters are consisted of 10 nm sized particles with very small sized pores and the pores between the clusters are observed to be large, about more than 100 nm.



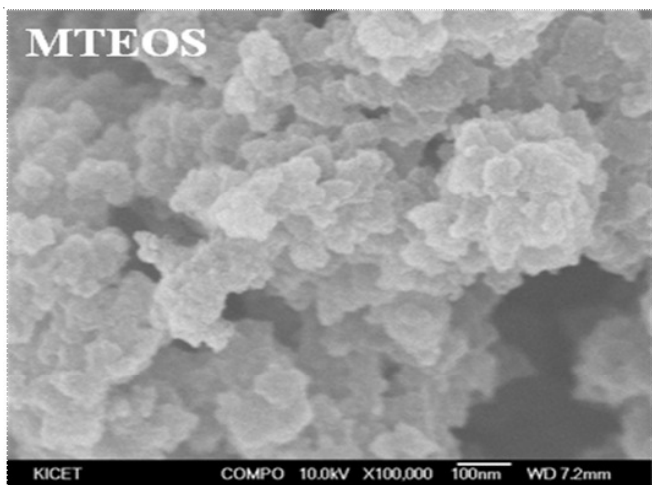
(a)

TABLE-2
PROPERTIES OF TEOS, TEOS/MTEOS AND MTEOS-BASED AEROGELS

Data sample	BET (m ² /g)	Pore volume (cc/g)	Pore size (Å)	Density (g/cm ³)	Porosity (%)
MTEOS	586	0.564	58-464	0.066	94.69
TEOS/MTEOS	1165	5.371	159	0.104	91.80
TEOS	1016	2.671	267	0.123	90.44



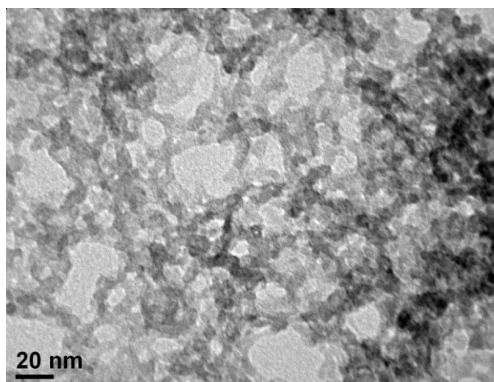
(b)



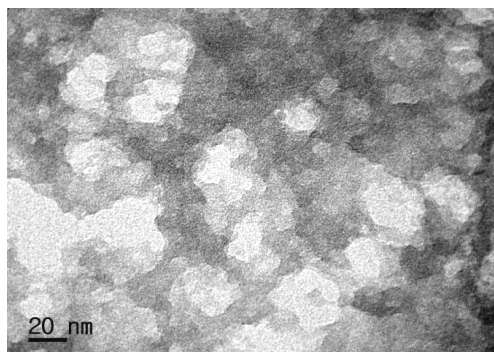
(c)

Fig. 6. SEM photographs of TEOS, TEOS/MTEOS and MTEOS-based silica aerogels

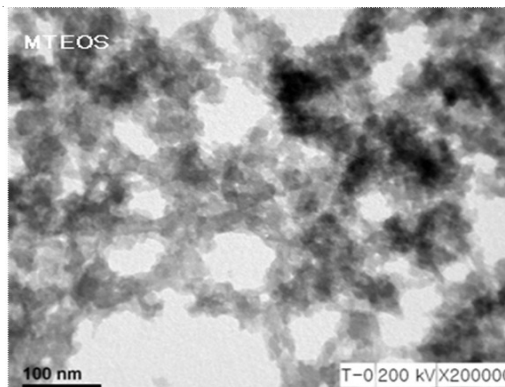
TEM images clearly showed the microstructures of TEOS, TEOS/MTEOS and MTEOS-based aerogels (Fig. 7). TEOS-based silica aerogels showed the very small sized porous structures, comprised of networks of about 10 nm sized particles. TEOS/MTEOS aerogels are observed to be consisted of two different-sized pores, large pores with 100 nm in diameter and small pores with less than 20 nm in diameter. MTEOS aerogels showed the microstructures with macropores more than 100 nm. MTEOS aerogels were consisted of networks of about 100 nm-sized clusters which contain of small particles and small pores less than 10 nm.



(a)



(b)



(c)

Fig. 7. TEM photographs of TEOS, TEOS/MTEOS and MTEOS-based silica aerogels

Mechanical strength and elastic modulus: Fig. 8 showed the mechanical strength and elastic modulus of TEOS, TEOS/MTEOS and MTEOS-based aerogels. TEOS-based aerogel showed the flexural strength, 64 kPa and its elastic modulus is 155 kPa. The flexural strength and elastic modulus of TEOS/MTEOS-based hybrid aerogel decreased to 55 and 93 kPa, respectively and further sharply led to 27 and 12 kPa for MTEOS-based aerogels.

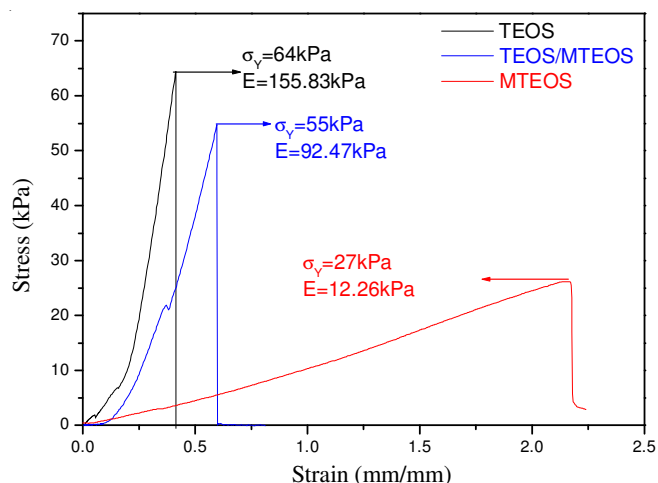


Fig. 8. Flexural Strength of TEOS, TEOS/MTEOS and MTEOS silica aerogels

Contact angles of hybrid aerogels: Fig. 9 showed the contact angles of hybrid aerogels with variations of MTEOS contents.

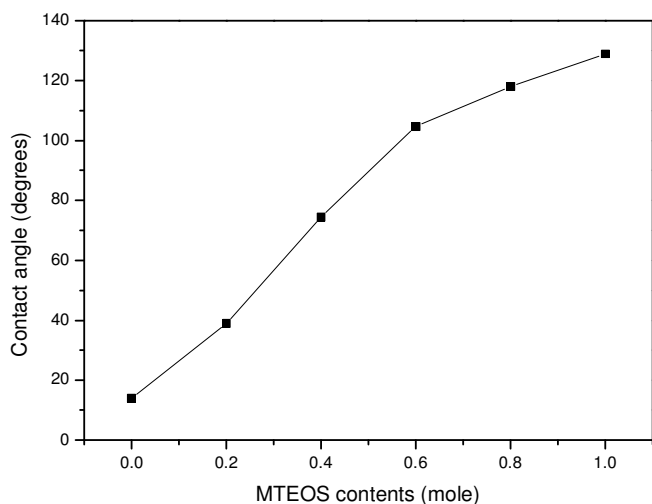


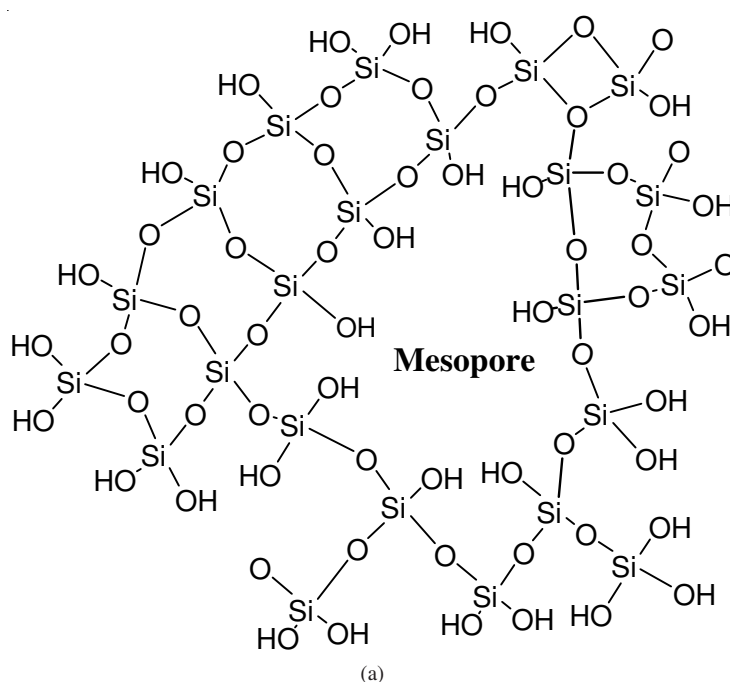
Fig. 9. Contact angles of Hybrid aerogels with varying MTEOS contents

The surface chemical modification by alkyl groups is a well-known method of lowering the surface energy of a solid and thereby making it highly water repellent, *i.e.*, superhydrophobic¹⁶. The MTEOS monomer ($\text{H}_3\text{C-Si}(\text{OC}_2\text{H}_5)_3$) contains a non-hydrolyzable methyl group ($-\text{CH}_3$) and the *in situ* modifications of CH_3 groups to the siloxane backbone during the sol-gel polymerization leads to very high solid-liquid interfacial energy, which in turn results in a superhydrophobic aerogel. Therefore, the increase of MTEOS contents linearly increased the contact angles from 14° for TEOS to 129° for MTEOS-based aerogels.

To control the flexibility of aerogel, we tried the hybridization of TEOS and MTEOS-based aerogels. The schematic diagram of TEOS, TEOS/MTEOS and MTEOS-based aerogels are presented in Fig. 10. TEOS-based aerogels are comprised of three dimensional networks of silica with hydroxyl groups on the pore surfaces which function as hydrophilic agent. So, TEOS-based aerogels synthesized by CO_2 supercritical method

show hydrophilic property. In addition, the network bones comprising TEOS-based aerogel are silica particles with about 10 nm in diameter that are hard and brittle. Therefore, TEOS-based silica aerogels are very brittle for they are comprised of more than ninety percent of pores. The network structure and pore size are affected by hydrolysis and condensation reactions of TEOS, which are greatly determined by $\text{H}_2\text{O}/\text{TEOS}$ ratio, quantities of catalyst, the kind of catalyst (acid or base), the kind of precursors and so on.

In this paper, we concentrated on the precursor effects, especially TEOS and MTEOS. Bhagat *et al.*¹⁶ synthesized MTMS-based aerogels with high flexibility caused by methyl functional group. Methyl functional group confers the flexibility and hydrophobicity. However, they only synthesized MTMS-based aerogels but did not characterize the pore structures and network structures of the aerogels. So, we focused on the hybridization of TEOS with four ethoxy functional groups and MTEOS with three ethoxy and one methyl functional groups. MTEOS is rather difficult to be hydrolyzed and condensed because of one methyl functional group. It could be linked in three directions with three ethoxy groups but could not have network formation in the direction of methyl functional group as is shown in Fig. 9(c). Therefore, very high concentration of basic catalyst, ammonia, needs to be added to MTEOS or MTMS sols to progress a gellation. It is inferred that MTEOS-based aerogels are more open structures with macropores because it is comprised of methyl functional groups that could not form the networks. The more difficult hydrolysis and condensation reactions of MTEOS due to methyl functional group needs higher concentration of basic catalyst, which also affects the network and pore structures. It is known that strong basic catalyst forms the networks of large particles with inner micropores. These effects caused by the methyl functional group confer the flexibility, hydrophobicity, macroporous structures of MTEOS-based aerogels.



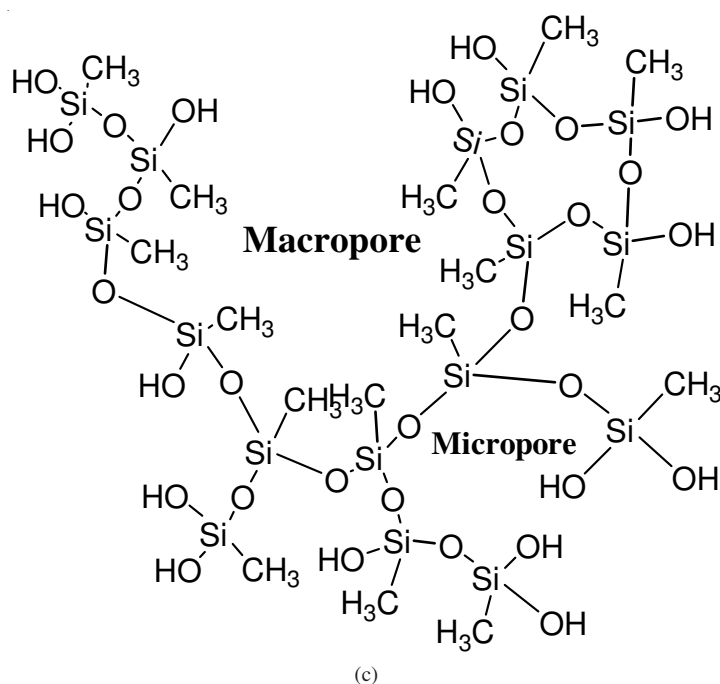
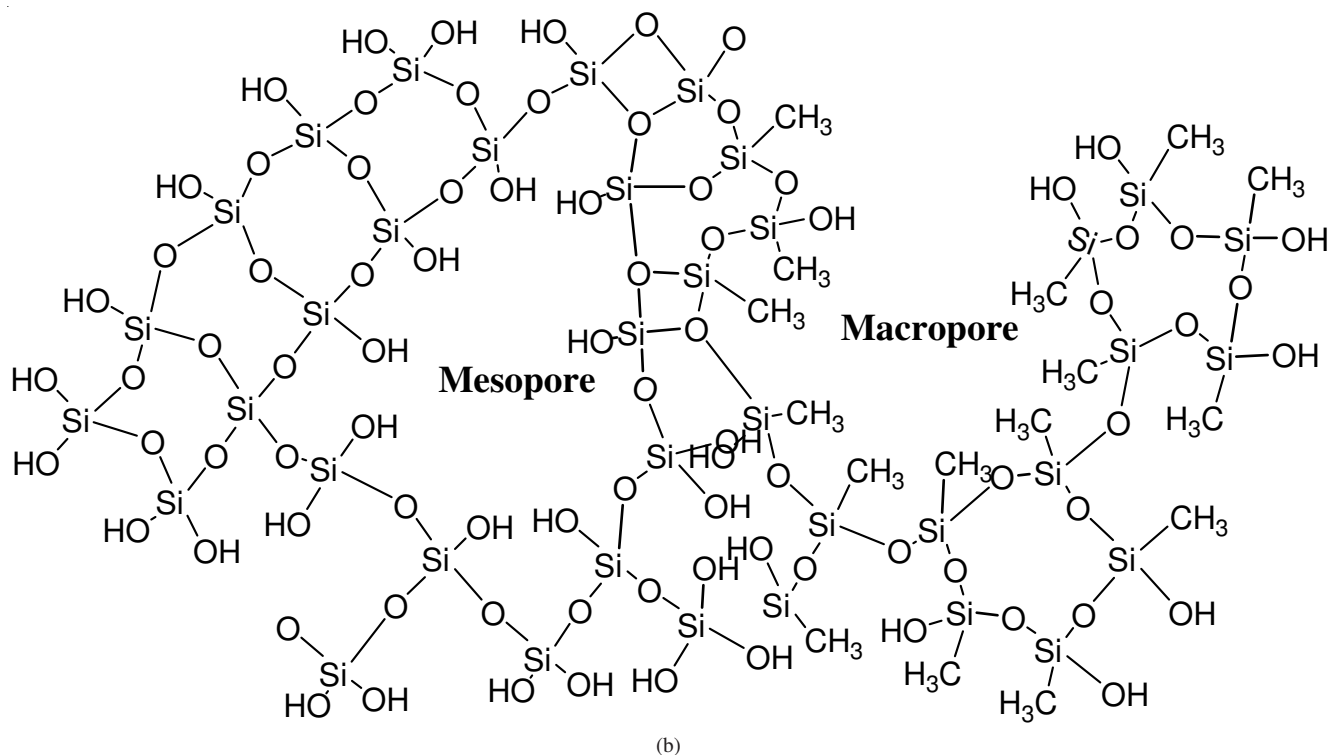


Fig. 10. TEOS, TEOS/MTEOS and MTEOS-based aerogel network schemes

However, MTEOS-based aerogels have very large pore structures and low specific area, although it has the advantages of flexibility and hydrophobicity. So, it is thought that the idea of hybridization of TEOS and MTEOS help to obtain flexible and hydrophobic aerogels with higher specific area than that of TEOS-based aerogels. The elongation of TEOS/MTEOS was 0.6, which increased from 0.4 for TEOS but was lower than 2.1 for MTEOS, which means that TEOS/MTEOS is brittle. However, we can control the flexibility of hybrid aerogels by changing the ratio of TEOS and MTEOS.

Conclusion

We found that the flexibility, pore structures such as pore sizes, porosity and specific surface area could be controlled by changing ratio of TEOS/MTEOS. A methyl functional group of MTEOS causes the difficulty of hydrolysis and condensation reactions, so that strong basic catalyst needs to be added for the gellation of MTEOS. Therefore, increasing of MTEOS ratio forms larger pore sizes and large primary particles with about one micrometer. MTEOS-based aerogels show the lowest specific area due to macropores with more

than 100 nm, although they are very flexible to elongate two times as long as their original sample length. For TEOS/MTEOS hybrid aerogels with 1:1 molar ratio, they have the largest specific surface area and pore volume, a little flexibility and hydrophobicity due to the remaining alkyl functional groups. This research presents the possibility of controlling flexibility, pore structures, hydrophobicity through hybridization of alkoxide and silane. It suggests a way of overcoming weaknesses of silica aerogels like brittleness and hydrophilicity.

ACKNOWLEDGEMENTS

The authors grateful for the financial supports by Strategic Research Program of Korea Institute of Cermaic Engineering & Technology and by a grant from the Fundamental R&D Program for Core Technology of Materials by the Ministry of Knowledge Economy, Republic of Korea Government.

REFERENCES

1. L.W. Hrubesh, *J. Non-Cryst. Solids*, **225**, 335 (1988).
2. S. Svendsen, *J. Non-Cryst. Solids*, **145**, 240 (1992).
3. V. Wittwer, *J. Non-Cryst Solids*, **145**, 233 (1992).
4. Z. Deng, J. Wang, A. Wu, J. Shen and B. Zhou, *J. Non-Cryst. Solids*, **225**, 101 (1998).
5. S. Kistler, *Nature*, **127**, 741 (1931).
6. A.E. Gash, J.H. Satcher Jr. and R.L. Simpson, *Chem. Mater.*, **15**, 3268 (2003).
7. M.A.B. Meadr, E.F. Fabrizio, F. Ilhan, A. Dass, G. Zhang, P. Vassilaras, J.C. Johnsein and N. Leventis, *Chem. Mater.*, **17**, 1085 (2005).
8. A.C. Pierre and G.M. Pajonk, *Chem. Rev.*, **102**, 4242 (2002).
9. X. Hu, K. Littrel, S. Ji, D.G. Pickles and W.M. Risen Jr., *J. Non-Cryst. Solids*, **288**, 184 (2001).
10. G.S. Kim and S.H. Hyun, *J. Mater Sci.*, **38**, 1961 (2003).
11. M.F. Bertino and J.F. Hund, *J. Sol-Gel Sci. Technol.*, **30**, 43 (2004).
12. S. Ramamurthi and M. Ramamurthi, US Patent 5,306,555 (1994).
13. S. Christopher, G. George and B. Redouna, WO 02 052086 (2002).
14. C.A. Morris, M.L. Anderson, R.M. Stroud, C.I. Merzbacher and D.R. Rolison, *Science*, **284**, 622 (1999).
15. A.V. Rao, S.D. Bhagat, H. Hirashima and G.M. Pajonk, *J. Colloid Interf. Sci.*, **300**, 279 (2006).
16. S.D. Bhagat, C.-S. Oh, Y.-H. Kim, Y.-S. Ahn and J.-G. Yeo, *Micropor. Mesopor. Mater.*, **100**, 350 (2007).
17. C.-Y. Kim, J.-K. Lee and B.-I. Kim, *Colloid. Surf. A Physicochem. Eng. Asp.*, **313-314**, 179 (2008).
18. C.-Y. Kim, J.-K. Lee and B.-I. Kim, *Mater. Sci. Forum.*, **544-545**, 673 (2007).
19. C.-Y. Kim, A.R. Jang, B.I. Kim and D.H. Suh, *J. Sol-Gel Sci. Technol.*, **48**, 336 (2008).
20. B. Cheng, L. Zhao, J. Yu and X. Zhao, *Mater. Res. Bull.*, **43**, 714 (2008).
21. R. Akkari, A. Ghorbel, N. Essayem and F. Figueras, *Appl. Catal. A Gen.*, **328**, 43 (2007).
22. C.J. Lee, G.S. Kim and S.H. Hyun, *J. Mater Sci.*, **37**, 2237 (2002).
23. C.J. Brinker and W.G. Scherer, *Sol-Gel Science: The Physics and Chemistry of Sol-Gel Processing*, Tokyo Academic Press, Boston, p. 583 (1990).
24. B. Riegel, I. Hartmann, W. Kiefer, J. Gros and J. Fricke, *J. Non-Cryst Solids*, **211**, 294 (1997).
25. B. Riegel, S. Plittersdorf, W. Keifer, N. Husing and U. Schubert, *J. Mol. Struct.*, **410-411**, 157 (1997).